

Cooperative Synchronization in Wireless Networks

Bernhard Etzlinger, *Student Member, IEEE*, Henk Wymeersch, *Member, IEEE*,
and Andreas Springer, *Member, IEEE*

Abstract—We consider networks where nodes differ in clock frequency and phase, and aim to synchronize to a master clock. Nodes exchange packets and are able to exchange and measure noisy time information. When the measurement noise is Gaussian, we propose two fully distributed, cooperative network synchronization algorithms. These algorithms are derived using belief propagation and mean field message passing, are shown to be convergent, and outperform a variety of competing algorithms. Our performance results are complemented by and compared with the relevant Bayesian Cramér–Rao bounds.

Index Terms—Network synchronization, Belief propagation, Mean field, Distributed estimation, Bayesian Cramér–Rao bound.

I. INTRODUCTION

SYNCHRONIZATION in wireless networks enables a number of important applications that rely on hard time constraints, such as distributed estimation or tracking [1], [2], time-division-multiple-access communication protocols [3], and cooperative transmission (e.g., distributed beamforming) [4]. These applications require a common notion of time, whereas each network node has its individual communication hardware and clock with individual timing behavior. These clocks are driven by oscillators, which, due to imperfections and environmental factors, may drift with respect to each other [5]. Hence, network nodes need to be synchronized to the extent required by the application.

Network synchronization schemes differ mainly in how local time information is encoded, exchanged, and processed [6]. We will limit ourselves to the so-called packet-coupled synchronization, whereby local time is encoded in time stamps and exchanged via packet transmissions [7]. Research in this area can be grouped into three broad fields: measurement protocols [7]–[9], performance bounds [10]–[14], and practical synchronization algorithms [8], [14]–[21]. Measurement protocols can be one-way or two-way [7], and can be distorted by deterministic and stochastic effects [8]. To reduce the effect of higher layers in the protocol stack, physical layer time-stamping can be used [9]. For a collection of measurements, fundamental performance bounds can be derived: considering a pair of nodes, Cramér–Rao bounds are derived in [12], [13], later extended to Bayesian Cramér–Rao and Chapman–Robbins bounds [10]. Further Cramér–Rao bounds have been

B. Etzlinger and A. Springer are with the Institute of Communications Engineering and RF-Systems, Johannes Kepler University, Linz, Austria, e-mail: {b.etzlinger, a.springer}@nths.jku.at. H. Wymeersch is with the Department of Signals and Systems, Chalmers University of Technology, Gothenburg, Sweden. email: henkw@chalmers.se.

This research was supported, in part, by the European Research Council, under Grant No. 258418 (COOPNET) and by the COMET K2 Center “Austrian Center of Competence in Mechatronics (ACCM)”. The COMET Program is funded by the Austrian Federal government, the Federal State of Upper Austria and the Scientific Partners of ACCM.

derived for star networks with a central master node in [11], and for general networks in [14]. However, these bounds do not consider available prior information on the unknown clock parameters.

Much of the recent work on packet-coupled synchronization has focused on practical synchronization algorithms, which either steer the clock parameters towards an average value, or achieve a common clock value imposed by a master. An average value can be attained through average consensus and its variations [15], [22] or alternating direction method of multiplier consensus [16], [17]. Alternatively, [18] uses additional constraints on the sum of relative clock parameters over cycles in the network to achieve a common clock value imposed by a master. A common drawback of these approaches is relatively slow convergence to the average value, especially for sparsely connected networks and in the presence of large outliers. In contrast, faster convergence in the presence of master nodes can be achieved when structure is imposed on the network: this can be a tree (e.g., for the flooding time synchronization protocol [8]) or a cluster (e.g., for reference broadcast synchronization [19]). Forming and maintaining the structure have an overhead cost, and make the network more sensitive to node failures. Moreover, nodes far away from the master exhibit degraded performance. Some of these drawbacks can be mitigated through centralized processing [14], [21]. There is thus a clear need for network synchronization algorithms that combine the best features of all these approaches: *fast* convergence, *distributed* processing, and *without network structure* limitations. To address this, [20] proposed a Bayesian algorithm based on belief propagation in a factor graph representation [23] of the problem, though only for a clock model where nodes have different clock phases. Unfortunately, the assumption of perfect clock frequencies is not reasonable for many practical applications, thus requiring frequent re-synchronization.

In this paper, we build on the work from [20], considering both relative clock phases and clock skews. Our contributions are as follows:

- Based on a real measurement model, we derive an approximate, yet accurate statistical model that allows a Gaussian reformulation of the maximum a posteriori estimation of clock parameters, enabling the development of computationally simple algorithms;
- We propose two fully distributed, cooperative synchronization algorithms based on message passing on a suitable factor graph. We demonstrate their convergence and their superior convergence rates, compared to state-of-the-art methods; and
- We derive a Bayesian Cramér–Rao bound (BCRB), which serves as a fundamental performance bound for the case

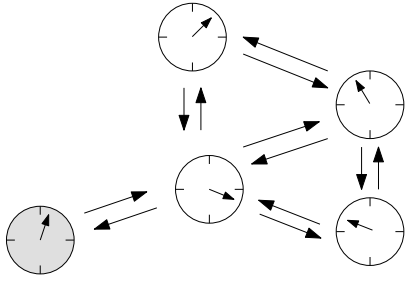


Figure 1. Connectivity graph of a wireless network with $M = 1$ master node (shaded) and $A = 4$ agent nodes.

when prior information on the local clock parameters is available.

The remainder of this paper is organized as follows: In Section II, we introduce the clock model, the network model, and the measurement protocol. In Section III, we provide an overview of the state-of-the-art on distributed synchronization, under both phase and skew uncertainties. Exact and simplified statistical models of measurement likelihoods and clock priors are derived in Section IV, followed by a description of the BCRB in Section V. The simplified models from Section IV are used to derive two Bayesian algorithms based on message passing in Section VI. In Section VII, we numerically study the properties of the proposed algorithms and compare them to state-of-the-art algorithms from Section III. Finally, we draw our conclusions in Section VIII.

II. SYSTEM MODEL

A. Network Model

We consider a network comprising a set \mathcal{M} of master nodes and a set \mathcal{A} of agent nodes (see Fig. 1). The $M = |\mathcal{M}| > 0$ fully synchronous master nodes impose a common time reference to the network. The $A = |\mathcal{A}|$ agent nodes have imperfect clocks that may not run synchronously with the reference time. Any node $i \in \mathcal{M} \cup \mathcal{A}$ is able to communicate with its neighbors $\mathcal{N}(i)$ in communication range from node i , where the communication is supposed to be bi-directional. All connections (i, j) are collected in the set of edges \mathcal{E} . The network is assumed to be connected, i.e., there is a path between every pair of nodes.

B. Clock Model

Each network node i possesses a clock displaying local time $c_i(t)$, related to the time reference (or true time) t by

$$c_i(t) = \alpha_i t + \beta_i, \quad (1)$$

where β_i is the clock phase of node i and α_i is the clock skew of node i [7]. When $i \in \mathcal{M}$, $\alpha_i = 1$ and $\beta_i = 0$. When $i \in \mathcal{A}$, both α_i and β_i are considered as random variables. The clock phase β_i depends on the initial network state, and can be modeled with an uninformative prior (e.g., as uniformly distributed over a large range, or, equivalently, having Gaussian distribution with a large variance $\sigma_{\beta,i}^2$ [20]). The clock skew α_i depends on the quality of the clocks, typically expressed in parts per million (ppm), and is modeled as a Gaussian

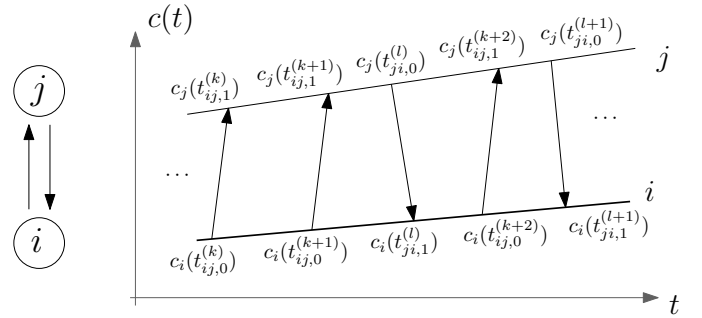


Figure 2. Time instants at a reference time t of the n -th two-way timing message exchange between node j and node i with the local clocks $c_j(t)$ and $c_i(t)$.

random variable [24] with mean 1 and variance $\sigma_{\alpha,i}^2$. Note that nodes with more sophisticated clocks will have smaller $\sigma_{\alpha,i}^2$. The following notation will be convenient: $\theta_i = [\alpha_i, \beta_i]^T$, $\theta_{ij} = [\theta_i^T, \theta_j^T]^T$, $\theta = [\theta_1^T, \dots, \theta_A^T]^T$, $\theta'_i = [1/\alpha_i, \beta_i/\alpha_i]^T$, $\theta'_{ij} = [(\theta'_i)^T, (\theta'_j)^T]^T$, and $\theta' = [(\theta'_1)^T, \dots, (\theta'_A)^T]^T$.

C. Measurement Model

Following [14], pairs of nodes $(i, j) \in \mathcal{E}$ exchange data packets with time stamps, as shown in Fig. 2. Node i transmits $K_{ij} \geq 1$ packets to node j and receives $K_{ji} \geq 1$ from node j . The k -th packet from node i is transmitted at time $t_{ij,0}^{(k)}$ and received by node j after a delay $\delta_{ij}^{(k)}$, at time

$$t_{ij,1}^{(k)} = t_{ij,0}^{(k)} + \delta_{ij}^{(k)}. \quad (2)$$

The nodes have only access to $c_j(t_{ij,1}^{(k)})$ and $c_i(t_{ij,0}^{(k)})$, which can be related to (2) through (1) as

$$c_j(t_{ij,1}^{(k)}) = \frac{c_i(t_{ij,0}^{(k)}) - \beta_i}{\alpha_i} \alpha_j + \beta_j + \delta_{ij}^{(k)} \alpha_j \quad (3)$$

for $k \in \{1, \dots, K_{ij}\}$. A similar relation holds for the packets sent by node j to node i , by exchanging i and j in (3). We will assume that transmit times $c_i(t_{ij,0}^{(k)})$ are recorded exactly, so that the aggregate observation between nodes i and j is given by

$$\mathbf{c}_{ij} = [\mathbf{c}_{i \rightarrow j}^T, \mathbf{c}_{j \rightarrow i}^T]^T$$

in which

$$\mathbf{c}_{i \rightarrow j} = [c_j(t_{ij,1}^{(1)}), c_j(t_{ij,1}^{(2)}), \dots, c_j(t_{ij,1}^{(K_{ij})})]^T.$$

The delay $\delta_{ij}^{(k)}$ can be broken up as $\delta_{ij}^{(k)} = \Delta_{ij} + w_{ij}^{(k)}$ [8], where Δ_{ij} is a deterministic component (related to coding and signal propagation) and $w_{ij}^{(k)}$ is a stochastic component. We model $\Delta_{ij} = T_c + T_{f,ij}$ as comprising a hardware related computation time T_c , and a time of flight $T_{f,ij}$. We further suppose that $\Delta_{ij} = \Delta_{ji}$. To model $w_{ij}^{(k)}$, we have performed a measurement campaign with two Texas Instruments ez430-RF2500 evaluation boards. We placed the boards 1 meter apart and transmitted 10,000 packets, collecting¹ the corresponding

¹Via the general debug output (GDO with GDOx_CFG = 6) of the CC2500 transceiver chip, time of transmission and time of reception was measured. Note that the GDO pins reference is valid for the concept of physical layer time-stamping [9].

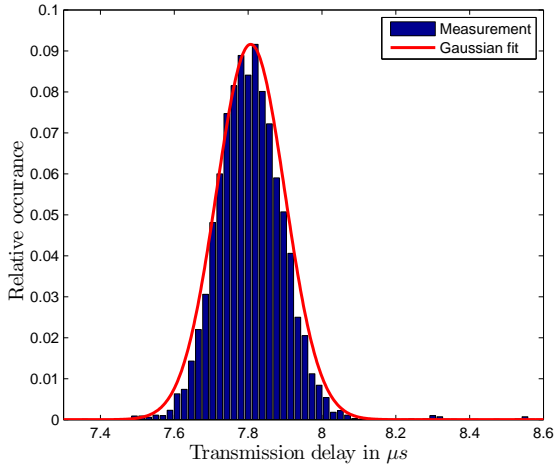


Figure 3. Measurement data and Gaussian fit of the delay $\delta_{ij}^{(k)} = \Delta_{ij} + w_{ij}^{(k)}$.

transmit $t_{i,j,0}^{(k)}$ and receive times $t_{i,j,1}^{(k)}$. Their measured difference on an oscilloscope reveals the delays $\delta_{ij}^{(k)}$ according to (2), shown as a histogram in Fig. 3. We conclude that a zero-mean Gaussian model for $w_{ij}^{(k)}$ is appropriate, which is congruent with the models from [7], [10]–[13]. We will denote the variance of the measurement noise $w_{ij}^{(k)}$ by σ_m^2 , for all $(i, j) \in \mathcal{E}$.

D. Network Synchronization

Our goal is to infer the local clock parameters α_i and β_i (or an invertible transformation thereof), based on the measurements and the prior clock information. In the following sections, we will describe standard approaches to solve this problem, followed by our proposed Bayesian approach.

III. STATE-OF-THE-ART

In this section, we briefly present existing synchronization methods for the presented clock and network model. We limit our overview to algorithms that perform parameter estimation based on time stamp exchange in a fully distributed manner, where every node runs the same algorithm. Within this class, we discuss approaches based on average consensus [15], alternating direction of multiplier method (ADMM) [17], and loop constrained combination of pairwise estimations [18].

A. Average TimeSync

Consensus protocols are based on averaging information received from neighbors, and thus have low computational complexity. Moreover, master nodes are not required and, if present, may lead to a decrease in convergence speed. In the Average TimeSync (ATS) algorithm from [15], every node has a virtual clock

$$\hat{c}_i(c_i(t)) = \hat{\alpha}_i c_i(t) + \hat{\beta}_i = \hat{\alpha}_i \alpha_i t + \hat{\alpha}_i \beta_i + \hat{\beta}_i,$$

which is controlled by a virtual skew $\hat{\alpha}_i$ and a virtual phase $\hat{\beta}_i$. By adjusting the virtual skew and phase, ATS assures asymptotic agreement on the virtual clocks $\lim_{t \rightarrow \infty} \hat{c}_i(c_i(t)) = \tau_v(t)$,

$\forall i \in \mathcal{A}$, where $\tau_v(t)$ is a network-wide common time. The algorithm assumes $\delta_{ij} = 0$.

B. ADMM Consensus

In ADMM consensus from [17], relative skews $\alpha_{ij} = \alpha_i / \alpha_j$ and relative phase offsets $\beta_{ij} = \beta_i - \beta_j$ are assumed to be available a priori (e.g., from an estimation algorithm such as [12]). Then follows a network-wide correction of the local clock parameters in discrete instances $k\Delta T$. Collecting the clock skews in $\mathbf{T}^{(k)} = [\alpha_1^{(k)} \Delta T, \dots, \alpha_A^{(k)} \Delta T]^T$, and the clock phases in $\boldsymbol{\beta}^{(k)} = [\beta_1^{(k)}, \dots, \beta_A^{(k)}]^T$, control signals $\mathbf{u}^{(k)}$ and $\mathbf{v}^{(k)}$ are applied as

$$\begin{aligned} \boldsymbol{\beta}^{(k+1)} &= \boldsymbol{\beta}^{(k)} + \mathbf{T}^{(k)} + \mathbf{u}^{(k)} \\ \mathbf{T}^{(k+1)} &= \mathbf{T}^{(k)} + \mathbf{v}^{(k)}. \end{aligned}$$

The computation of $v_i^{(k)}$ at a node i is based on ADMM and requires knowledge of α_{jk} for all nodes $j \in \mathcal{N}(i), k \in \mathcal{N}(j)$, i.e., from all two-hop neighbors. It can be shown that as $k \rightarrow +\infty$, $\mathbf{T}^{(k)} \rightarrow \bar{T} \cdot \mathbf{1}_{A,1}$ for some common value \bar{T} , where $\mathbf{1}_{k,l}$ denotes a $k \times l$ matrix with all entries equal to one. Finally, agreement on the clock phases is achieved through the control signal $\mathbf{u}^{(k)}$ using average consensus. Although fully distributed and master-free, ADMM consensus requires inner iterations for offset measurements and outer iterations for the consensus. It further relies on a step size parameter, whose optimal value depends on global network properties.

C. Loop Constrained Synchronization

In [18], it was observed that for every closed loop \mathcal{L} in the network, it is such that $\sum_{i,j \in \mathcal{L}} \tilde{x}_{ij} = 0$, for $\tilde{x}_{ij} = \beta_i - \beta_j$ and $\tilde{x}_{ij} = \log(\alpha_i / \alpha_j)$. Using these constraints, the absolute clock values are determined via coordinate descent of the least squares problem [18]

$$\hat{\mathbf{v}} = \arg \min_{\mathbf{v}} \|\mathbf{A}\mathbf{v} - \tilde{\mathbf{x}}\|^2,$$

where \mathbf{A} is the incidence matrix representing a directed topology, \mathbf{v} the vector of absolute clock parameters (phase or skew) and $\tilde{\mathbf{x}}$ is the collection of offset measurements. In order to find a global optimum, a master node needs to be selected. During the iterations, local estimates on absolute skew and phase are exchanged with all one-hop neighbors.

IV. STATISTICAL MODELS

The above-mentioned algorithms are all non-Bayesian, and thus do not fully exploit all statistical information present in the network. When clock skews are known, fast, distributed Bayesian algorithms were derived in [20]. When clock skews are unknown, the naive extension of [20] would lead to impractical algorithms, due to the complex integrals that need to be computed. In this section, we propose a series of approximations to measurement likelihoods and prior distributions, with the aim of a simple representation of the posterior distribution. Using this simplifications, the maximum a posteriori (MAP) estimate of the clock parameters (or a transformation thereof) can be found with reasonable complexity.

A. Likelihood Function

For every pair of nodes, there is a local likelihood function $p(\mathbf{c}_{ij}|\boldsymbol{\theta}_{ij}; \Delta_{ij})$, which due to the conditional independence of the measurements, can be factorized as

$$\begin{aligned} p(\mathbf{c}_{ij}|\boldsymbol{\theta}_{ij}; \Delta_{ij}) & \quad (4) \\ &= (2\pi\alpha_i^2\sigma_m^2)^{-K_{ij}/2} \exp\left(-\frac{\|\mathbf{c}_{i\rightarrow j} - \mathbf{F}_{i\rightarrow j}(\boldsymbol{\theta}_{ij}, \Delta_{ij})\|^2}{2\alpha_i^2\sigma_m^2}\right) \\ &\times (2\pi\alpha_j^2\sigma_m^2)^{-K_{ji}/2} \exp\left(-\frac{\|\mathbf{c}_{j\rightarrow i} - \mathbf{F}_{j\rightarrow i}(\boldsymbol{\theta}_{ij}, \Delta_{ij})\|^2}{2\alpha_j^2\sigma_m^2}\right), \end{aligned}$$

where $\mathbf{F}_{i\rightarrow j}(\boldsymbol{\theta}_{ij}, \Delta_{ij})$ is obtained by stacking $(c_i(t_{ij,0}^{(k)} - \beta_i)\alpha_j/\alpha_i + \beta_j + \Delta_{ij}\alpha_j)$, which is the deterministic part from (3), in a column vector of length K_{ij} . Observe that (4) is difficult to work with, since (i) the factor outside the exponential depends on α_i and α_j ; and (ii) the dependence on the unknown delay Δ_{ij} .

The first problem can be avoided by approximating $(2\pi\alpha_i^2\sigma_m^2)^{-K_{ij}/2}$ by $(2\pi\sigma_m^2)^{-K_{ij}/2}$, which leads a good approximation of (4), as long as the clock skews are close to one, which is the physically relevant case. We deal with the second problem by computing the maximum likelihood estimate of Δ_{ij} and substituting the estimate back into the likelihood. Taking the logarithm of (4) and setting the derivative with respect to Δ_{ij} to zero leads to the following estimate

$$\hat{\Delta}_{ij}(\boldsymbol{\theta}_{ij}) = a_i \frac{1}{\alpha_i} + a_j \frac{1}{\alpha_j} + b_{ij} \frac{\beta_i}{\alpha_i} - b_{ij} \frac{\beta_j}{\alpha_j}, \quad (5)$$

where a_i, a_j, b_{ij} are functions of the observations, detailed in Appendix A. Substituting (5) in (4) and considering the approximation of the normalization constant leads to the following approximate likelihood function

$$\tilde{p}(\mathbf{c}_{ij}|\boldsymbol{\theta}'_{ij}) \propto \exp\left(-\frac{1}{2\sigma_m^2} \|\mathbf{A}_{ij}\boldsymbol{\theta}'_i + \mathbf{B}_{ij}\boldsymbol{\theta}'_j\|^2\right), \quad (6)$$

with

$$\begin{aligned} \mathbf{A}_{ij} &= \begin{bmatrix} -c_i(t_{ij,0}^{(1)}) & 1 \\ \vdots & \vdots \\ -c_i(t_{ij,0}^{(K_{ij})}) & 1 \\ c_i(t_{ji,1}^{(1)}) & -1 \\ \vdots & \vdots \\ c_i(t_{ji,1}^{(K_{ji})}) & -1 \end{bmatrix} + [a_i \quad +b_{ij}] \otimes \mathbf{1}_{K_{ij}+K_{ji},1}, \\ \mathbf{B}_{ij} &= \begin{bmatrix} c_j(t_{ij,1}^{(1)}) & -1 \\ \vdots & \vdots \\ c_j(t_{ij,1}^{(K_{ij})}) & -1 \\ -c_j(t_{ji,0}^{(1)}) & 1 \\ \vdots & \vdots \\ -c_j(t_{ji,0}^{(K_{ji})}) & 1 \end{bmatrix} + [a_j \quad -b_{ij}] \otimes \mathbf{1}_{K_{ij}+K_{ji},1}, \end{aligned}$$

where \otimes denotes the Kronecker product. The approximated likelihood function in (6) no longer contains the delay Δ_{ij} and

can be interpreted as Gaussian in the transformed parameters $\boldsymbol{\theta}'_{ij}$. As we will see in Section VI, this latter observation has advantages in the algorithm design for distributed parameter estimation since it leads to simpler computation rules.

B. Prior Information

Since our simplified likelihood function now has a Gaussian form in the transformed clock parameters $\boldsymbol{\theta}'_{ij}$, we need to select a suitable Gaussian prior so as to end up with a Gaussian posterior distribution. We will choose

$$p(\boldsymbol{\theta}'_i) = \mathcal{N}_{\boldsymbol{\theta}'_i}(\boldsymbol{\mu}_{p,i}, \boldsymbol{\Sigma}_{p,i}), \quad (7)$$

where $\mathcal{N}_{\mathbf{x}}(\boldsymbol{\mu}, \boldsymbol{\Sigma})$ denotes a Gaussian distribution in \mathbf{x} with mean vector $\boldsymbol{\mu}$ and covariance matrix $\boldsymbol{\Sigma}$. For master nodes, we have perfect knowledge of skew and phase, so we set

$$\boldsymbol{\mu}_{p,i} = \begin{bmatrix} 1 \\ 0 \end{bmatrix}, \quad \boldsymbol{\Sigma}_{p,i} = \begin{bmatrix} a & 0 \\ 0 & a \end{bmatrix}, \quad a \rightarrow 0 \quad \text{for } i \in \mathcal{M}. \quad (8)$$

For agent nodes, we use the prior information on the clock skews from the local oscillator specification. Denoting $\alpha_i = 1 + \varepsilon_i$ with $|\varepsilon_i| \ll 1$, it follows that $1/\alpha_i = 1/(1 + \varepsilon_i) \approx 1 - \varepsilon_i$, so $\mathbb{E}\{1/\alpha_i\} \approx 2 - \mathbb{E}\{\alpha_i\} = 1$ and $\mathbb{E}\{1/\alpha_i^2\} - \mathbb{E}\{1/\alpha_i\}^2 \approx \mathbb{E}\{\alpha_i^2\} - \mathbb{E}\{\alpha_i\}^2 = \sigma_{\alpha,i}^2$. Under our assumption of an uninformative prior on β_i , it follows that β_i/α_i can also be modeled with an uninformative prior. Hence, we find

$$\boldsymbol{\mu}_{p,i} = \begin{bmatrix} 1 \\ 0 \end{bmatrix}, \quad \boldsymbol{\Sigma}_{p,i} \approx \begin{bmatrix} \sigma_{\alpha,i}^2 & 0 \\ 0 & \sigma_{\beta,i}^2 \end{bmatrix} \quad \text{for } i \in \mathcal{A}, \quad (9)$$

where $\sigma_{\beta,i}^2 \gg \sigma_{\alpha,i}^2$.

C. Posterior Distribution and Estimator

Putting together the approximate likelihood function from Section IV-A with the prior in the transformed parameters from Section IV-B, we find the following posterior distribution in the transformed parameters

$$\tilde{p}(\boldsymbol{\theta}'|\mathbf{c}) \propto \prod_{i \in \mathcal{A} \cup \mathcal{M}} p(\boldsymbol{\theta}'_i) \prod_{(i,j) \in \mathcal{E}} \tilde{p}(\mathbf{c}_{ij}|\boldsymbol{\theta}'_{ij}), \quad (10)$$

which is a Gaussian distribution in $\boldsymbol{\theta}'$. The inverse covariance matrix $\tilde{\boldsymbol{\Sigma}}^{-1}$ of this Gaussian turns out to be highly structured, with block entries (for $i, j \in \mathcal{A}$)

$$\begin{aligned} [\tilde{\boldsymbol{\Sigma}}^{-1}]_{i,i} &= \boldsymbol{\Sigma}_{p,i}^{-1} + \sum_{j \in \mathcal{N}(i)} \frac{1}{\sigma_m^2} \mathbf{A}_{ij}^T \mathbf{A}_{ij} + \frac{1}{\sigma_m^2} \mathbf{B}_{ji}^T \mathbf{B}_{ji} \\ [\tilde{\boldsymbol{\Sigma}}^{-1}]_{i,j} &= \begin{cases} \frac{1}{\sigma_m^2} \mathbf{A}_{ij}^T \mathbf{B}_{ij} + \frac{1}{\sigma_m^2} \mathbf{B}_{ji}^T \mathbf{A}_{ji} & \text{for } j \in \mathcal{N}(i) \\ \mathbf{0} & \text{else.} \end{cases} \quad (11) \end{aligned}$$

If we are able to marginalize $\tilde{p}(\boldsymbol{\theta}'|\mathbf{c})$ to recover $\tilde{p}(\boldsymbol{\theta}'_i|\mathbf{c})$, we can compute the MAP estimate of $\boldsymbol{\theta}'_i$, $i \in \mathcal{A}$ as

$$\begin{aligned} \hat{\boldsymbol{\theta}}'_i &= \arg \max_{\boldsymbol{\theta}'_i} \tilde{p}(\boldsymbol{\theta}'_i|\mathbf{c}) \\ &= \arg \max_{\boldsymbol{\theta}'_i} \int \tilde{p}(\boldsymbol{\theta}'|\mathbf{c}) d\boldsymbol{\theta}'_i, \end{aligned} \quad (12)$$

where $\boldsymbol{\theta}'_i$ indicates that the integration is over all $\boldsymbol{\theta}'_j$ except $\boldsymbol{\theta}'_i$. From $\hat{\boldsymbol{\theta}}'_i$ we can further determine the clock parameters by $\hat{\alpha}_i = 1/[\hat{\boldsymbol{\theta}}'_i]_1$ and $\hat{\beta}_i = [\hat{\boldsymbol{\theta}}'_i]_2/[\hat{\boldsymbol{\theta}}'_i]_1$, where $[\cdot]_m$ extracts the m -th element of a vector. Solving this problem in a distributed manner will be the topic of Section VI.

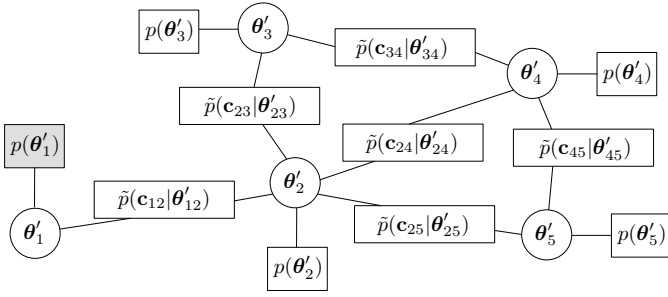


Figure 4. Factor graph of the posterior distribution for a 5 node network with $\mathcal{M} = \{1\}$ and $\mathcal{A} = \{2, 3, 4, 5\}$.

V. BAYESIAN CRAMÉR–RAO BOUND

Based on the statistical models from Section IV, it is possible to derive fundamental performance bounds on the quality of estimators. One such bound is the BCRB, which gives a lower bound on the achievable estimation accuracy on θ_i [25]. The BCRB is derived based on the Fisher information matrix, assuming known Δ_{ij} for every link:

$$\begin{aligned} \mathbf{J} &= -\mathbb{E}_{\theta, \mathbf{c}} \left[\left\{ \nabla_{\theta} \{ \nabla_{\theta} [\log p(\theta | \mathbf{c}; \Delta)] \}^T \right\} \right] \\ &= -\mathbb{E}_{\theta, \mathbf{c}} \left[\left\{ \nabla_{\theta} \{ \nabla_{\theta} [\log p(\mathbf{c} | \theta; \Delta)] \}^T \right\} \right] \\ &\quad - \mathbb{E}_{\theta} \left[\left\{ \nabla_{\theta} \{ \nabla_{\theta} [\log p(\theta)] \}^T \right\} \right] \\ &= \mathbb{E}_{\theta} [\mathbf{J}_p] + \mathbb{E}_{\theta} [\mathbf{J}_l], \end{aligned} \quad (13)$$

in which the matrix \mathbf{J}_p represents the contribution of the prior information, and is a diagonal matrix with block entries equal to the covariances matrices in (9). The matrix \mathbf{J}_l represents the contribution of the likelihood function $p(\mathbf{c} | \theta; \Delta) = \mathcal{N}_{\mathbf{c}}(\boldsymbol{\mu}_l, \boldsymbol{\Sigma}_l)$, which is the product of the pairwise functions in (4). It is computed as

$$[\mathbf{J}_l]_{i,j} = \frac{\partial \boldsymbol{\mu}_l^T}{\partial \theta_i} \boldsymbol{\Sigma}_l^{-1} \frac{\partial \boldsymbol{\mu}_l}{\partial \theta_j} + \frac{1}{2} \text{trace} \left[\boldsymbol{\Sigma}_l^{-1} \frac{\partial \boldsymbol{\Sigma}_l}{\partial \theta_i} \boldsymbol{\Sigma}_l^{-1} \frac{\partial \boldsymbol{\Sigma}_l}{\partial \theta_j} \right] \quad (14)$$

for $i, j \in \mathcal{A}$. \mathbf{J}_l has 2×2 non-zero blocks in the main diagonal and in i -th row and j -th column when $j \in \mathcal{N}(i)$. Thus, it will have the same structure as the inverse covariance matrix in (11). Additional details are provided in Appendix B. Finally, the BCRB on a certain parameter, say the k -th parameter in the $2A$ -dimensional vector θ , is given by

$$\text{BRCB}_k = [\mathbf{J}^{-1}]_{k,k}.$$

VI. DISTRIBUTED PARAMETER ESTIMATION

To solve the marginalization in (12) in a distributed way, we use approximate inference via message passing on factor graphs. In the following, we describe the factor graph for the synchronization problem and motivate the use of message passing for optimum retrieval of posterior marginals. Finally, we derive two synchronization algorithms.

A. Factor Graph

The factor graph associated to the factorization in (10) is found by drawing a variable vertex for every variable (drawn as circles) and a factor/function vertex for every factor (drawn as

rectangles). Vertices are connected via edges according to their functional dependencies. The factor graph² that corresponds to the connectivity graph in Fig. 1 is depicted in Fig. 4. Note that every variable vertex corresponds to the variables of a physical network node and that every factor vertex corresponds to a measurement link in the physical network. Thus, the structure of the connectivity graph is kept in the factor graph: a tree connectivity remains as tree factor graph, a star connectivity remains as star factor graph, and so on.

Factor graphs are combined with message passing methods in order to compute, e.g., marginal posteriors. Different message passing methods lead to different performance/complexity trade-offs. A framework to compare message passing method is found through variational free energy minimization.

B. Energy Minimization for Marginal Retrieval

Our goal is to find practical methods to determine, exactly or approximately, the marginals from (12). From [27], one strategy is to minimize the *variational free energy* for a positive function $b(\theta')$ approximating $\tilde{p}(\theta' | \mathbf{c})$:

$$b^*(\cdot) = \arg \min_{b(\cdot)} \int b(\theta') \log \frac{b(\theta')}{\tilde{p}(\theta' | \mathbf{c})} d\theta'. \quad (15)$$

As algorithm designers, we can impose structure to the function $b(\theta')$ to allow efficient solving of (15). We will consider two classes of functions: (i) the Bethe method, in which $b(\theta')$ is constrained to be a product of factors of the form $b_i(\theta'_i)$ and $b_{ij}(\theta'_i, \theta'_j)$; and (ii) the mean field method, which constrains $b(\theta')$ to be of the form $b(\theta') = \prod_i b_i(\theta'_i)$. Minimizing (15) subject to the constraints imposed by the approximations, leads to the message passing rules [27]. The message passing rules turn out to be the belief propagation (BP) equations for class (i) and the mean field (MF) equations for class (ii).

In the following we use the shorthand p_{ij} for $\tilde{p}(\mathbf{c}_{ij} | \theta'_{ij})$. Furthermore, since the approximated joint posterior distribution in (10) is Gaussian in θ' , we consider only messages that are Gaussian in θ' .

C. Synchronization by Message Passing

Above we motivated two message passing schemes, BP and MF. By applying both, we find two synchronization algorithms where network nodes cooperate by the exchange of messages. We now present the algorithms in detail, and discuss their salient properties. A unified view of the message passing is offered in Fig. 5.

1) *Belief Propagation*: The BP message from a factor vertex p_{ij} to a variable vertex θ'_i is given by [23, Eq. (6)]

$$\begin{aligned} m_{p_{ij} \rightarrow \theta'_i}(\theta'_i) &= \int p_{ij}(\theta'_{ij}) m_{\theta'_j \rightarrow p_{ij}}(\theta'_j) d\theta'_j \\ &\propto \mathcal{N}_{\theta'_i}(\boldsymbol{\mu}_{\text{in},ij}, \boldsymbol{\Sigma}_{\text{in},ij}), \end{aligned} \quad (16)$$

²The representation differs slightly from the factor graph presented in [20], as in our case both nodes have access to the same function vertex since they share the measurements. The presentation in [20] accounts for 2 disjoint sets of measurements that are not shared between the nodes [26].

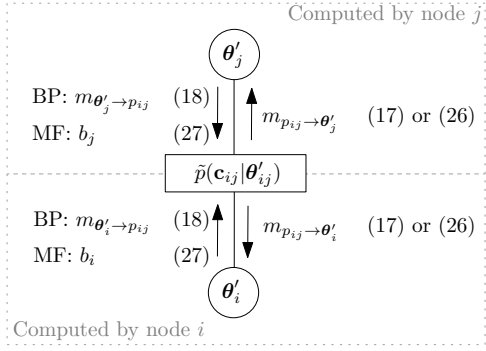


Figure 5. Messages between a node pair i, j of a general network. Since the measurements are shared, both nodes have access to the same function vertex.

while the BP message from a variable vertex θ'_i to a factor vertex p_{ij} is given by [23, Eq. (5)]

$$m_{\theta'_i \rightarrow p_{ij}}(\theta'_i) = p(\theta'_i) \prod_{k \in \{N(i) \setminus j\}} m_{p_{ik} \rightarrow \theta'_i}(\theta'_i) \propto \mathcal{N}_{\theta'_i}(\boldsymbol{\mu}_{\text{ext},ij}, \boldsymbol{\Sigma}_{\text{ext},ij}), \quad (17)$$

where we use the index “in” for intrinsic and “ext” for extrinsic with respect to a variable vertex. As depicted in Fig. 5, each network node i corresponding to the variable vertex θ'_i needs to compute its intrinsic and extrinsic message. Furthermore, note that for BP, the extrinsic message $m_{\theta'_i \rightarrow p_{ij}}$ has to be determined separately for every node $j \in N(i)$. For message computation, the parameter updates (for detailed derivations, see Appendix C) of (16) are, if the neighboring node is an agent, $j \in N(i) \cap \mathcal{A}$

$$\mathbf{Q} = \frac{1}{\sigma_m^2} \mathbf{A}_{ij}^T \mathbf{B}_{ij} (\mathbf{B}_{ij}^T \mathbf{B}_{ij} + \sigma^2 \boldsymbol{\Sigma}_{\text{ext},ji}^{-1})^{-1}$$

$$\boldsymbol{\Sigma}_{\text{in},ij}^{-1} = \frac{1}{\sigma_m^2} \mathbf{A}_{ij}^T \mathbf{A}_{ij} - \mathbf{Q} \mathbf{B}_{ij}^T \mathbf{A}_{ij} \quad (18)$$

$$\boldsymbol{\Sigma}_{\text{in},ij}^{-1} \boldsymbol{\mu}_{\text{in},ij} = -\mathbf{Q} \boldsymbol{\Sigma}_{\text{ext},ji}^{-1} \boldsymbol{\mu}_{\text{ext},ji}, \quad (19)$$

and if the neighboring node is a master, $j \in N(i) \cap \mathcal{M}$

$$\boldsymbol{\Sigma}_{\text{in},ij}^{-1} = \frac{1}{\sigma_m^2} \mathbf{A}_{ij}^T \mathbf{A}_{ij} \quad (20)$$

$$\boldsymbol{\Sigma}_{\text{in},ij}^{-1} \boldsymbol{\mu}_{\text{in},ij} = -\frac{1}{\sigma_m^2} \mathbf{A}_{ij}^T \mathbf{B}_{ij} \boldsymbol{\mu}_{\text{ext},ji}. \quad (21)$$

The parameter updates of (17) are

$$\boldsymbol{\Sigma}_{\text{ext},ij}^{-1} = \boldsymbol{\Sigma}_{p,i}^{-1} + \sum_{k \in \{N(i) \setminus j\}} \boldsymbol{\Sigma}_{\text{in},ki}^{-1} \quad (22)$$

$$\boldsymbol{\Sigma}_{\text{ext},ij}^{-1} \boldsymbol{\mu}_{\text{ext},ij} = \boldsymbol{\Sigma}_{p,i}^{-1} \boldsymbol{\mu}_{p,i} + \sum_{k \in \{N(i) \setminus j\}} \boldsymbol{\Sigma}_{\text{in},ki}^{-1} \boldsymbol{\mu}_{\text{in},ki}. \quad (23)$$

The approximate marginal is obtained by

$$b_i(\theta'_i) \propto p(\theta'_i) \prod_{k \in N(i)} m_{p_{ik} \rightarrow \theta'_i}(\theta'_i) \propto \mathcal{N}_{\theta'_i}(\boldsymbol{\mu}_i, \boldsymbol{\Sigma}_i). \quad (24)$$

The parameters of the marginal belief (24) are computed from the parameters in (22) and (23), but with the additional summation over j .

In the communication between two connected nodes i and j as in Fig. 5, node i transmits $m_{\theta'_i \rightarrow p_{ij}}$ to j and vice versa. The receiving node then computes its intrinsic message to the variable vertex (e.g., node j computes $m_{p_{ij} \rightarrow \theta'_j}$). As a node i has evaluated the intrinsic messages from all its neighbors, it can determine again its extrinsic messages. After I iterations, every node i computes the marginal belief $b_j(\theta'_j)$ and thereof the MAP estimates of its clock parameters.

2) *Mean Field*: The MF message from a factor vertex p_{ij} to a variable vertex θ'_i is given by [28, Eq. (14)]

$$m_{p_{ij} \rightarrow \theta'_i}(\theta'_i) = \exp \left(\int \log(p_{ij}(\theta'_{ij})) b_j(\theta'_j) d\theta'_j \right) \propto \mathcal{N}_{\theta'_i}(\boldsymbol{\mu}_{\text{in},ij}, \boldsymbol{\Sigma}_{\text{in},ij}), \quad (25)$$

and the message from a variable vertex θ'_i to a factor vertex p_{ij} is given by the belief [28, Eq. (16)]

$$b_i(\theta'_i) \propto p(\theta'_i) \prod_{k \in N(i)} m_{p_{ik} \rightarrow \theta'_i}(\theta'_i) \propto \mathcal{N}_{\theta'_i}(\boldsymbol{\mu}_i, \boldsymbol{\Sigma}_i). \quad (26)$$

The corresponding parameter updates (for detailed derivations, see Appendix D) are

$$\boldsymbol{\Sigma}_{\text{in},ij}^{-1} = \frac{1}{\sigma_m^2} \mathbf{A}_{ij}^T \mathbf{A}_{ij} \quad (27)$$

$$\boldsymbol{\Sigma}_{\text{in},ij}^{-1} \boldsymbol{\mu}_{\text{in},ij} = \frac{1}{\sigma_m^2} \mathbf{A}_{ij}^T \mathbf{B}_{ij} \boldsymbol{\mu}_j \quad (28)$$

and

$$\boldsymbol{\Sigma}_i^{-1} = \boldsymbol{\Sigma}_{p,i}^{-1} + \sum_{k \in N(i)} \boldsymbol{\Sigma}_{\text{in},ki}^{-1} \quad (29)$$

$$\boldsymbol{\Sigma}_i^{-1} \boldsymbol{\mu}_i = \boldsymbol{\Sigma}_{p,i}^{-1} \boldsymbol{\mu}_{p,i} + \sum_{k \in N(i)} \boldsymbol{\Sigma}_{\text{in},ki}^{-1} \boldsymbol{\mu}_{\text{in},ki}. \quad (30)$$

For MF, two connected nodes (i, j) only need to exchange their beliefs instead of extrinsic information (see Fig. 5). Since the same information is sent to all neighbors, this can also be performed in a broadcast scheme. From the belief, the receiver then can compute the intrinsic message (25).

3) *Belief Propagation vs. Mean Field*: We now discuss the difference between both methods with respect to convergence and computational complexity.

- **Convergence** BP computes the true marginals if the factor graph is a tree. If the factor graph has cycles, this can not be guaranteed in general. However, for joint Gaussian distributions, as in our case for (10), sufficient conditions for convergence exist. Furthermore, if Gaussian BP converges, it is known that it converges to the true mean value [29]. Popular convergence conditions are diagonal dominance [29] or walk-summability [30], which can be evaluated via the information matrix (11). It turns out that diagonal dominance, while easy to check³, is not fulfilled for (10). In contrast, the walk-sum condition is difficult to prove for a general setting as it requires the spectral radius

³The absolute value of the main diagonal element in the information matrix of (10) must be larger than the sum of the absolute values of the remaining entries in the same row.

of the block transformed information matrix. However, numerical evaluation revealed that the condition is always fulfilled for the used simulation settings. In contrast to BP, MF always converges [31, pp. 466]. Furthermore, MF converges to the true mean vector for Gaussian graphical models [32, pp.136].

- **Computational complexity** The BP rules are computationally more complex, as can be observed by comparing (18) and (19) with (27) and (28). Moreover, BP requires the computation of an extrinsic message towards every single neighbor, i.e., for BP (17) has to be computed for every neighbor per iteration whereas (26) has to be computed only once per iteration.

D. Scheduling and Implementation Aspects

In this section, we discuss message scheduling and ways to efficiently combine timing information exchange and message passing in real applications.

We consider a general topology as in Fig. 4. Every node $i \in \mathcal{A}$ runs the same algorithm, and computes the message parameters to/from the function vertices as depicted in Fig. 5. Therefore, the node requires $m_{\theta'_j \rightarrow p_{ij}}(\theta'_j)$ to compute $m_{p_{ij} \rightarrow \theta'_i}(\theta'_i)$. Together with the prior information, the node then computes the outgoing message $m_{\theta'_i \rightarrow p_{ij}}(\theta'_i)$, which is sent to neighbor j for the next iteration. In order to start this procedure, all $m_{\theta'_j \rightarrow p_{ij}}(\theta'_j)$ in the factor graph have to be initialized. This can be done by setting them to uniform distributions, with mean value zero and infinite covariance.

In order to improve convergence speed, we use a flooding schedule, where a node only propagates if it has a significant belief on its parameters. Hence, in the first iteration only master nodes $m \in \mathcal{M}$ propagate messages. In the second iteration, also their neighbors $j \in \mathcal{N}(m)$ will send messages, in the third their neighbors' neighbors and so on.

Finally, our derivations were based on the assumption that measurements were collected first, and then message passing was carried out. Since both phases rely on the exchange of packets between nodes, it is possible to combine them, thereby increasing the number of measurements as message passing iterations progress. Such piggybacking is beneficial in real applications. In order to successfully start the algorithm, a minimum number of measurement packets has to be exchanged between every node pair to provide initial timing information. This is due to the required matrix inversions in the message parameter computations.

E. Comparison with State-of-the-Art Algorithms

We will now describe the main similarities and differences of BP and MF to the previously described state-of-the-art algorithms from Section III. We will use the shorthand: ATS is Average TimeSync from [15], ADMM is the method proposed in [17], and LC is the loop constraint method from [18]. In Table I, we compare the algorithms according to the following criteria: if masters are required/supported (“Master support”), if the algorithm can work on unknown topology (“Unknown top.”), and if the synchronization is applicable for broadcast protocols (“Broadcast”). Moreover, we compare the number

Table I
COMPARISON OF ALGORITHMS

	ATS [15]	ADMM [17]	LC [18]	BP	MF
Master support	–	–	+	+	+
Unknown top.	+	–	+	+	+
Broadcast	+	–	+	–	+
Inf. dist. (hops)	1	2	1	1	1
Delay sensitivity	–	+	+	+	+
Low complexity	++	+	~	--	–

of hops required to pass packets for information computation (“Inf. dist.”), if the algorithm is insensitive to propagation delays $\delta_{ij} \neq 0$ (“Delay sensitivity”), and if the algorithm achieves the clock parameter estimation with low computational complexity (“Low complexity”). The last measure is evaluated by the runtime of the computer simulation. We grade the agreement to the topics with: very good (++), good(+), medium (~), low (–), very low (––).

We note that ADMM and BP can not be used in protocols that rely on broadcasts, since the exchanged synchronization information is different for every neighbor. Additionally, in order to compute outgoing information, ADMM requires the collection of timing information from neighbors in 2 hop distance, as compared to 1 hop for all other algorithms. The number of hops is directly related to the number of packet exchanges before new estimation updates can be performed. We also observe that BP and MF suffer from higher complexity, whereas they are competitive in all other respects: they are not sensitive to propagation delays and support an arbitrary number of synchronous master nodes. Between BP and MF, MF has the advantage that it supports broadcast protocols.

The remaining question regarding the estimation accuracy is addressed in the following section, where a superior behavior of BP and MF is observed.

VII. NUMERICAL ANALYSIS

A. Simulation Settings

If not specified otherwise, we use the delay and noise setting from the measurements in Fig. 3. In particular, the noise standard deviation is $\sigma_m = 93$ ns and the deterministic delay $\Delta_{ij} = T_c + T_{f,ij}$ comprises a computational time $T_c = 7.6$ μ s and the flight time $T_{f,ij} = d_{ij}/v$, where d_{ij} is the distance between nodes i and j , and v is the speed of light. Simulations are carried out on 50 random networks where $M = 1$ master nodes and $A = 9$ agent nodes are uniformly placed in a 100 m \times 100 m square area. Each node has a communication radius of 50 m which determines the connectivity of the network. An example topology is shown in Fig. 6. We further select $K_{ij} = K_{ji}$ between all node pairs, where a measurement from node i to node j is always followed with a measurement from node j to node i . The time between two subsequent measurements is set to 10 ms. The clock skews are drawn from a normal distribution corresponding to a 100 ppm specification, $\alpha_i \sim \mathcal{N}(1, 10^{-8})$, which represents the prior distribution. The clock phases are drawn from a uniform distribution in the interval $[-10, +10]$ s, where the Gaussian prior was specified with zero mean and a standard deviation of $\sigma_{\beta,i} = 5.8$ s. In the following we will use the root mean square error as performance measure, denoted by “RMSE of phase”

and ‘‘RMSE of skew’’. Since not all competing algorithms rely on a master node, the RMSE to the true clock parameters is not a meaningful measure in a direct comparison. Thus, for algorithms not supporting master nodes, the RMSE is evaluated with respect to the network’s mean error of skew and phase. Errorbars indicate the variation that arise from different network realizations.

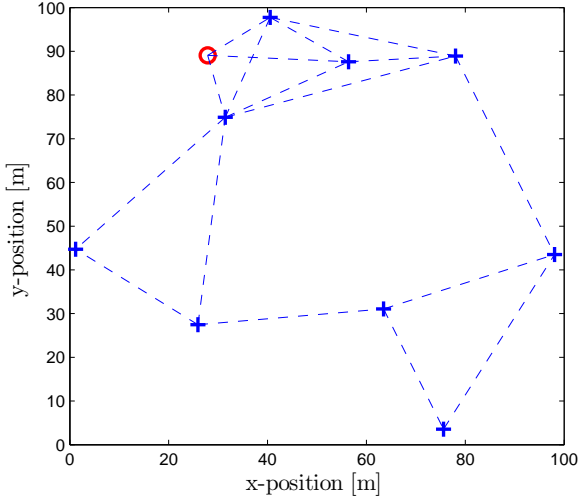


Figure 6. Randomly connected network with $M = 1$ (circle) and $A = 9$ (cross).

B. Study of BP and MF Synchronization

1) *Convergence*: Recall that MF will always converge, while BP is guaranteed to converge when the walk-sum condition [30] holds. Mathematically, this translates to

$$\rho(\mathbf{I} - \mathbf{S} \tilde{\Sigma}^{-1} \mathbf{S}^T) < 1, \quad (31)$$

where $\tilde{\Sigma}^{-1}$ is the information matrix from (10), \mathbf{S} is any block invertible transformations, and $\rho(\cdot)$ returns the spectral radius of its argument. Applying an eigenvalue decomposition to

$$[\tilde{\Sigma}^{-1}]_{i,i} = \mathbf{V} \mathbf{\Lambda} \mathbf{V}^T,$$

with eigenvectors \mathbf{V} and eigenvalues on the diagonal of $\mathbf{\Lambda}$, we use the block-diagonal transformation

$$[\mathbf{S}]_{i,i} = \mathbf{\Lambda}^{-1/2} \mathbf{V}^T.$$

We confirmed that (31) was satisfied for the following large parameter space:

- Number of nodes $M \in [5, 100]$;
- Noise variance $\sigma_m^2 \in [10^{-20}, 10^{-10}] \text{ s}^2$;
- Time between two measurements⁴ $T_r \in [0.01, 1] \text{ s}$;
- Computation time $T_c \in [0, 0.5] \text{ s}$;
- Communication range $r \in [50, 100] \text{ m}$; and
- Number of measurements $K_{ij} + K_{ji} \in [2, 620]$.

The most significant influence was observed by varying the number of measurements. With standard settings, this can be observed in Fig. 7.

⁴As response time we define $T_r = |t_{ij,0}^{(k)} - t_{ij,0}^{(l)}|$, where the instant l and k are two subsequent events.

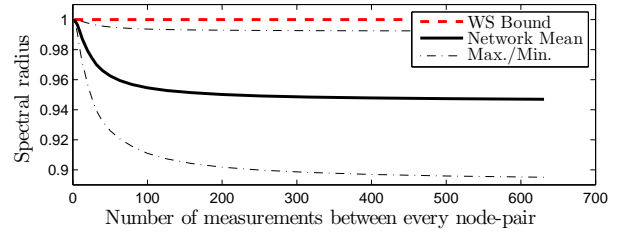


Figure 7. Condition for convergence: Spectral radius of transformed information matrix, $\rho(\mathbf{I} - \mathbf{S} \tilde{\Sigma}^{-1} \mathbf{S}^T)$, its variations of 50 network realizations and the walk-summability (WS) bound. In all cases, the criterion (31) was satisfied, so convergence of BP is guaranteed.

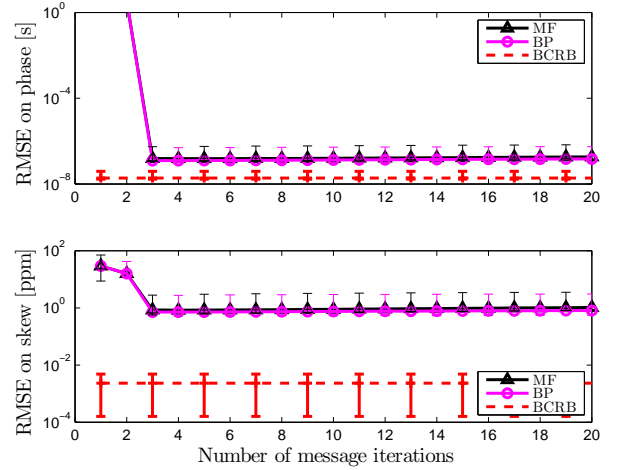


Figure 8. Convergence of parameter estimates with 7 measurements.

2) *Convergence Rate*: In Fig. 8, we show the BP and MF mean square error of the phase and skew estimates as a function of the iteration index. We observed that both algorithms converge after a number of iterations that correspond to the largest multi-hop distance of a node to a master node.⁵ Furthermore, both algorithms converge to the same values. The gap between estimation accuracy and BCRB arises due to the estimation of the transformed parameters θ' instead of the original parameters θ .

From the convergence analysis we can conclude, that the algorithms converge for practical relevant settings in a speed which can be predicted by the topology.

3) *Impact of Measurements*: Here, we vary the noise variance and the number of measurements, and provide results after $I = 7$ message passing iterations. In both cases, we observed that BP and MF gave rise to very similar results.

The variation of the number of measurements is depicted in Fig. 9, where the estimation results are compared to the BCRB. With the number of measurements the estimation accuracy increases and the gap to the BCRB is reduced.

Varying the noise variance σ_m^2 in Fig. 10 reveals its linear dependence to the estimation accuracy in double logarithmic scale. Both plots can be used as design criteria for the synchronization system.

⁵For the topology depicted in Fig. 6, which is part of the randomly generated topologies, the largest multi-hop distance is 4. This observation corresponds with the results shown by the simulation in Fig. 8.

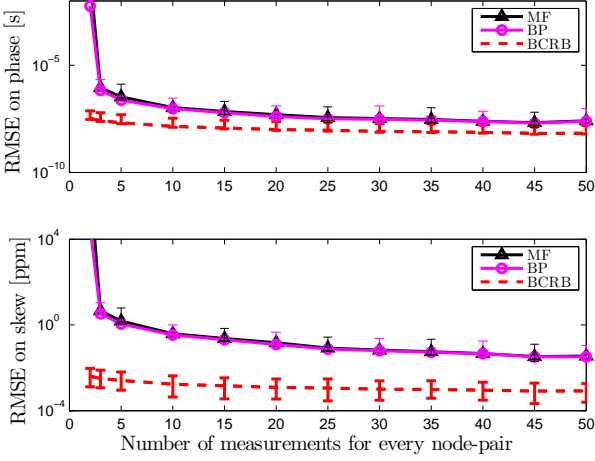


Figure 9. Variation of number of time measurements between every node pair with noise standard deviation $\sigma_m = 9.3 \cdot 10^{-8}$ s.

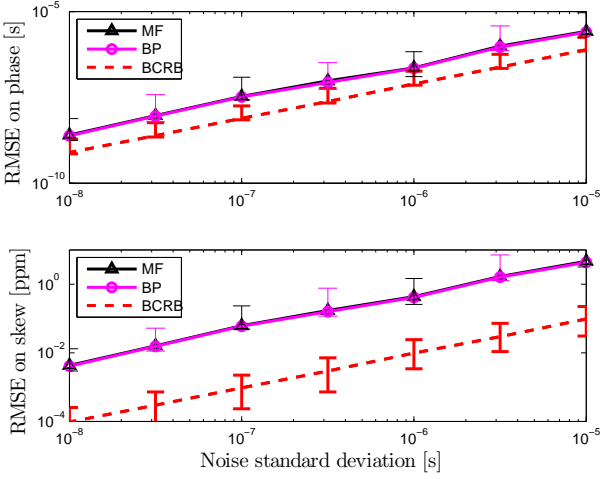


Figure 10. Variation of measurement noise between every node pair with 40 measurements.

C. Comparison to other Algorithms

We now compare BP and MF to other fully distributed state-of-the-art algorithms⁶ from Section III. Since in those methods time information and synchronization information exchange is interleaved, we apply the concept of piggybacking, introduced in Section VI-D. Furthermore, for a fair comparison, we set the computational delay $T_c = 0$ s, since not all methods account for deterministic delays between the nodes. Thus, the delay reduces to the time of flight, which is in the order of tenths of microseconds.

In Fig. 11 and Fig. 12, simulation results for phase and skew estimation are shown. The simulations were performed on the fixed network topology as depicted in Fig. 6 and the results are averaged over 50 runs. For both phase and skew estimation, the proposed algorithms outperform the competing ones for

⁶The following algorithm parameters are selected for [15]: filter values $\rho_\eta = \rho_\alpha = \rho_o = 0.6$; for [17]: step size ϵ_{opt} according to [17, Eq. (12)], relative skew estimation as in [12] with $K_{ij} = K_{ji} = 5$; and for [18]: filter parameter $\lambda = 0.9$.

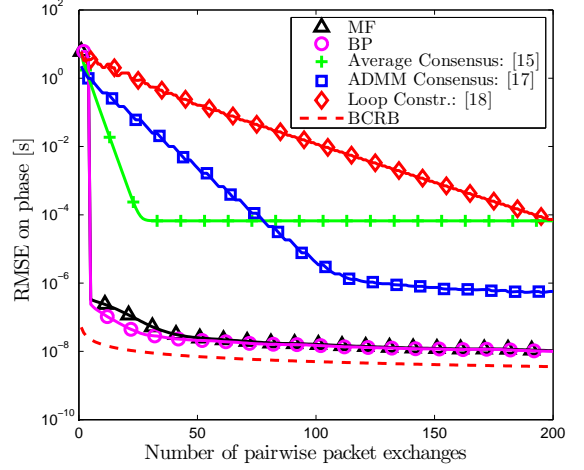


Figure 11. Root MSE of phase estimates for competing methods.

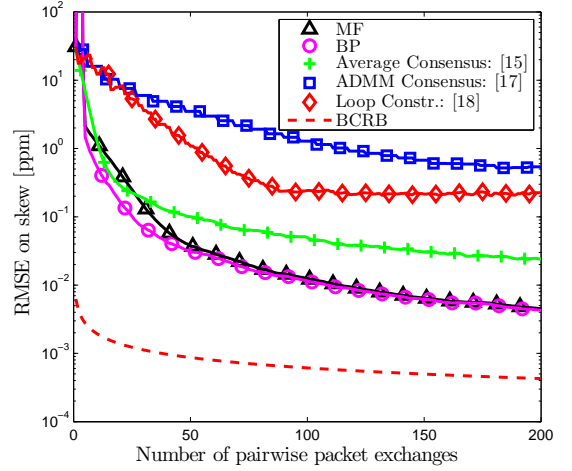


Figure 12. Root MSE of skew estimates for competing methods.

a fixed number of exchanged packets. Despite having higher complexity, we can conclude that the proposed algorithms have superior estimation performance and convergence speed compared to the other methods.

VIII. CONCLUSIONS

In this paper, we presented two cooperative and fully distributed network synchronization algorithms, which can be utilized when the measurement noise is (approximately) Gaussian. Using standard communication hardware, this approximation was verified by measurements. The synchronization algorithm design is based on message passing in a factor graph representation of the statistical model. Belief propagation (BP) and mean field (MF) message passing were applied to perform MAP estimation of the local clock parameters. We studied convergence, convergence rate, and accuracy, and found that in all three criteria, BP and MF are able to outperform existing algorithms. However, our results are in some cases still far away from a newly derived Bayesian CRB, indicating the possibility for further improvement.

APPENDIX

A. ML-estimate of the delay

The ML estimate of Δ_{ij} is given by

$$\hat{\Delta}_{ij} = \arg \max_{\Delta_{ij}} \log p(\mathbf{c}_{ij} | \boldsymbol{\theta}_{ij}; \Delta_{ij}),$$

where

$$\log p(\mathbf{c}_{ij} | \boldsymbol{\theta}_{ij}; \Delta_{ij}) \propto - \frac{\|\mathbf{c}_{i \rightarrow j} - \mathbf{F}_{i \rightarrow j}(\boldsymbol{\theta}_{ij}, \Delta_{ij})\|^2}{2\alpha_i^2 \sigma_m^2} - \frac{\|\mathbf{c}_{j \rightarrow i} - \mathbf{F}_{j \rightarrow i}(\boldsymbol{\theta}_{ij}, \Delta_{ij})\|^2}{2\alpha_j^2 \sigma_m^2}.$$

Since $\mathbf{F}_{i \rightarrow j}(\boldsymbol{\theta}_{ij}, \Delta_{ij})$ is linear in Δ_{ij} , taking the derivative of $\log p(\mathbf{c}_{ij} | \boldsymbol{\theta}_{ij}; \Delta_{ij})$ with respect to Δ_{ij} and equating the result to zero, immediately yields

$$\begin{aligned} \hat{\Delta}_{ij}(\boldsymbol{\theta}'_{ij}) &= \underbrace{\frac{K_{ij} \bar{c}_{i,ij} - K_{ji} \bar{c}_{i,ji}}{K_{ij} + K_{ji}}}_{a_i} \frac{1}{\alpha_i} \\ &+ \underbrace{\frac{-K_{ij} \bar{c}_{j,ij} + K_{ji} \bar{c}_{j,ji}}{K_{ij} + K_{ji}}}_{a_j} \frac{1}{\alpha_j} \\ &+ \underbrace{\frac{K_{ji} - K_{ij}}{K_{ij} + K_{ji}}}_{b_{ij}} \frac{\beta_i}{\alpha_i} + \underbrace{\frac{K_{ij} - K_{ji}}{K_{ij} + K_{ji}}}_{-b_{ij}} \frac{\beta_j}{\alpha_j}, \end{aligned} \quad (32)$$

with the averaged time stamps $\bar{c}_{i,ij} = 1/K_{ij} \sum_k c_i(t_{ij,0}^{(k)})$, $\bar{c}_{i,ji} = 1/K_{ji} \sum_l c_i(t_{ji,1}^{(l)})$ of i , and $\bar{c}_{j,ji} = 1/K_{ji} \sum_l c_j(t_{ji,0}^{(l)})$, $\bar{c}_{j,ij} = 1/K_{ij} \sum_k c_j(t_{ij,1}^{(k)})$ of j .

B. Computation of Fischer Information Matrix

1) *Computation of \mathbf{J}_l* : From the true likelihood (4) we have the parameter set $\boldsymbol{\Sigma}_l^{-1}, \boldsymbol{\mu}_l$ for every connected node pair (i, j) as

$$\begin{aligned} \boldsymbol{\mu}_{l,ij} &= [\mathbf{F}_{i \rightarrow j}(\boldsymbol{\theta}_{ij}, \Delta_{ij})^T \quad \mathbf{F}_{j \rightarrow i}(\boldsymbol{\theta}_{ij}, \Delta_{ij})^T]^T \\ \boldsymbol{\Sigma}_{l,ij} &= \begin{bmatrix} \alpha_i^2 \sigma_m^2 \mathbf{I}_{K_{ij}, K_{ij}} & \mathbf{0} \\ \mathbf{0} & \alpha_j^2 \sigma_m^2 \mathbf{I}_{K_{ji}, K_{ji}} \end{bmatrix}, \end{aligned}$$

where $\mathbf{I}_{k,l}$ denotes a $k \times l$ identity matrix. Applying (14) leads to the symmetric main diagonal block entries

$$\begin{aligned} [\mathbf{J}_l]_{i,i} &= \frac{1}{\sigma_m^2} \sum_{j \in \mathcal{N}(i)} \sum_{k=1}^{K_{ij}} \begin{bmatrix} \frac{(\phi_{ij,1}([\boldsymbol{\theta}'_i]_2))^2}{[\boldsymbol{\theta}'_i]_1^4} & \frac{\phi_{ij,1}([\boldsymbol{\theta}'_i]_2)}{[\boldsymbol{\theta}'_i]_1^3} \\ \frac{\phi_{ij,1}([\boldsymbol{\theta}'_i]_2)}{[\boldsymbol{\theta}'_i]_1^3} & \frac{1}{[\boldsymbol{\theta}'_i]_1^2} \end{bmatrix} \\ &+ \sum_{l=1}^{K_{ji}} \begin{bmatrix} \frac{\phi_{ji,2}(\boldsymbol{\theta}'_j)^2 + 2\sigma_m^2}{[\boldsymbol{\theta}'_j]_1^2} & \frac{\phi_{ji,2}([\boldsymbol{\theta}'_j]_2)}{[\boldsymbol{\theta}'_j]_1^2} \\ \frac{\phi_{ji,2}(\boldsymbol{\theta}'_j)}{[\boldsymbol{\theta}'_j]_1^2} & \frac{1}{[\boldsymbol{\theta}'_j]_1^2} \end{bmatrix}, \end{aligned}$$

where $\phi_{ij,1}([\boldsymbol{\theta}'_i]_2) = c_i(t_{ij,0}^{(k)}) - [\boldsymbol{\theta}'_i]_2$ and $\phi_{ij,2}(\boldsymbol{\theta}'_i) = \frac{c_i(t_{ij,0}^{(l)}) - [\boldsymbol{\theta}'_i]_2}{[\boldsymbol{\theta}'_i]_1} + \Delta_{ij}$ for any pair $(i, j) \in \mathcal{E}$. The off-diagonal

block entries are

$$\begin{aligned} [\mathbf{J}_l]_{i,j} &= - \frac{1}{\sigma_m^2} \sum_{k=1}^{K_{ij}} \begin{bmatrix} \frac{\phi_{ij,1}([\boldsymbol{\theta}'_i]_2) \phi_{ij,2}(\boldsymbol{\theta}'_i)}{[\boldsymbol{\theta}'_i]_1^2 [\boldsymbol{\theta}'_j]_1} & \frac{\phi_{ij,1}([\boldsymbol{\theta}'_i]_2)}{[\boldsymbol{\theta}'_i]_1^2 [\boldsymbol{\theta}'_j]_1} \\ \frac{\phi_{ij,2}(\boldsymbol{\theta}'_i)}{[\boldsymbol{\theta}'_i]_1 [\boldsymbol{\theta}'_j]_1} & \frac{1}{[\boldsymbol{\theta}'_i]_1 [\boldsymbol{\theta}'_j]_1} \end{bmatrix} + \\ &\sum_{l=1}^{K_{ji}} \begin{bmatrix} \frac{\phi_{ji,1}([\boldsymbol{\theta}'_j]_2) \phi_{ji,2}(\boldsymbol{\theta}'_j)}{[\boldsymbol{\theta}'_j]_1^2 [\boldsymbol{\theta}'_i]_1} & \frac{\phi_{ji,1}([\boldsymbol{\theta}'_j]_2)}{[\boldsymbol{\theta}'_j]_1^2 [\boldsymbol{\theta}'_i]_1} \\ \frac{\phi_{ji,2}(\boldsymbol{\theta}'_j)}{[\boldsymbol{\theta}'_j]_1 [\boldsymbol{\theta}'_i]_1} & \frac{1}{[\boldsymbol{\theta}'_j]_1 [\boldsymbol{\theta}'_i]_1} \end{bmatrix}^T \end{aligned}$$

for $j \in \mathcal{N}(i)$ and $[\mathbf{J}_l]_{i,j} = \mathbf{0}$ else.

2) *Expectations of $\mathbb{E}_\theta[\mathbf{J}_l]$ and $\mathbb{E}_\theta[\mathbf{J}_p]$* : The expectations $\mathbb{E}_\theta[\mathbf{J}_l]$ and $\mathbb{E}_\theta[\mathbf{J}_p]$ have to be taken over the inverse clock skews, i.e. $\mathbb{E}_\theta[1/\alpha_i^n]$, for n up to 4. Since the clock skews are Gaussian distributed and close to one, we use the approximations

$$\begin{aligned} \mathbb{E}\{1/\alpha_i\} &\approx 2 - \mu_{\alpha,i} & \mathbb{E}\{1/\alpha_i^2\} &\approx \sigma_{\alpha,i}^2 + \mathbb{E}\{1/\alpha_i\}^2 \\ \mathbb{E}\{1/\alpha_i^3\} &\approx \mathbb{E}\{1/\alpha_i\}^3 + 3 \mathbb{E}\{1/\alpha_i\} \sigma_{\alpha,i}^2 \\ \mathbb{E}\{1/\alpha_i^4\} &\approx \mathbb{E}\{1/\alpha_i\}^4 + 6 \mathbb{E}\{1/\alpha_i\}^2 \sigma_{\alpha,i}^2 + 3 \sigma_{\alpha,i}^4. \end{aligned}$$

C. Belief Propagation Update Rules

Derivation of the message parameters for $m_{p_{ij} \rightarrow \boldsymbol{\theta}'_i}(\boldsymbol{\theta}_i)$ in (16):

$$\begin{aligned} m_{p_{ij} \rightarrow \boldsymbol{\theta}'_i}(\boldsymbol{\theta}'_i) &= \int p_{ij}(\boldsymbol{\theta}'_{ij}) m_{\boldsymbol{\theta}'_j \rightarrow p_{ij}}(\boldsymbol{\theta}'_j) d\boldsymbol{\theta}'_j \\ &\propto \int \exp\left(-\frac{1}{2\sigma_m^2} \|\mathbf{A}_{ij} \boldsymbol{\theta}'_i + \mathbf{B}_{ij} \boldsymbol{\theta}'_j\|^2\right) \times \\ &\quad \mathcal{N}_{\boldsymbol{\theta}'_j}(\boldsymbol{\mu}_{\text{ext},ji}, \boldsymbol{\Sigma}_{\text{ext},ji}) d\boldsymbol{\theta}'_j \\ &= \exp\left(\frac{G_i(\boldsymbol{\theta}'_i)}{2}\right) \int \exp\left(\frac{G_{ij}(\boldsymbol{\theta}'_i, \boldsymbol{\theta}'_j)}{2}\right) d\boldsymbol{\theta}'_j \\ &\propto \exp\left(\frac{G_i(\boldsymbol{\theta}_i)}{2}\right) \\ &\propto \mathcal{N}_{\boldsymbol{\theta}'_i}(\boldsymbol{\mu}_{\text{in},ij}, \boldsymbol{\Sigma}_{\text{in},ij}). \end{aligned}$$

The functions $G_i(\boldsymbol{\theta}'_i)$ and $G_{ij}(\boldsymbol{\theta}'_i, \boldsymbol{\theta}'_j)$ are given by the exponent

$$\begin{aligned} & - \frac{1}{\sigma_m^2} \left(\boldsymbol{\theta}'_j{}^T \mathbf{B}_{ij}^T \mathbf{B}_{ij} \boldsymbol{\theta}'_j + 2 \boldsymbol{\theta}'_i{}^T \mathbf{A}_{ij}^T \mathbf{B}_{ij} \boldsymbol{\theta}'_j + \boldsymbol{\theta}'_i{}^T \mathbf{A}_{ij}^T \mathbf{A}_{ij} \boldsymbol{\theta}'_i \right) \\ & - \left(\boldsymbol{\theta}'_j - \boldsymbol{\mu}_{\text{ext},ji} \right)^T \boldsymbol{\Sigma}_{\text{ext},ji}^{-1} \left(\boldsymbol{\theta}'_j - \boldsymbol{\mu}_{\text{ext},ji} \right) \\ & = G_i(\boldsymbol{\theta}'_i) + G_{ij}(\boldsymbol{\theta}'_i, \boldsymbol{\theta}'_j) \end{aligned}$$

with

$$\begin{aligned} G_{ij}(\boldsymbol{\theta}'_i, \boldsymbol{\theta}'_j) &= - \left(\boldsymbol{\theta}'_j - \boldsymbol{\mu}' \right)^T \boldsymbol{\Sigma}'^{-1} \left(\boldsymbol{\theta}'_j - \boldsymbol{\mu}' \right) \\ & - \boldsymbol{\mu}_{\text{ext},ji}^T \boldsymbol{\Sigma}_{\text{ext},ji}^{-1} \boldsymbol{\mu}_{\text{ext},ji} \\ G_i(\boldsymbol{\theta}'_i) &= - \frac{1}{\sigma_m^2} \boldsymbol{\theta}'_i{}^T \underbrace{\left(\mathbf{A}_{ij}^T \mathbf{A}_{ij} - \mathbf{A}_{ij}^T \mathbf{B}_{ij} \frac{1}{\sigma_m^2} \boldsymbol{\Sigma}' \mathbf{B}_{ij}^T \mathbf{A}_{ij} \right)}_{\boldsymbol{\Sigma}_{\text{in},ij}^{-1}} \boldsymbol{\theta}'_i \\ & - \frac{2}{\sigma_m^2} \boldsymbol{\theta}'_i{}^T \underbrace{\mathbf{A}_{ij}^T \mathbf{B}_{ij} \frac{1}{\sigma_m^2} \boldsymbol{\Sigma}' \boldsymbol{\Sigma}_{\text{ext},ji}^{-1} \boldsymbol{\mu}_{\text{ext},ji}}_{\boldsymbol{\Sigma}_{\text{in},ij}^{-1} \boldsymbol{\mu}_{\text{ext},ji}} \end{aligned}$$

and

$$\begin{aligned}\Sigma'^{-1} &= \frac{1}{\sigma_m^2} (\mathbf{B}_{ij}^T \mathbf{B}_{ij} + \sigma_m^2 \Sigma_{\text{ext},ji}^{-1}) \\ \boldsymbol{\mu}' &= \Sigma' \left(\Sigma_{\text{ext},ji}^{-1} \boldsymbol{\mu}_{\text{ext},ji} + \frac{1}{\sigma_m^2} \mathbf{B}_{ij}^T \mathbf{A}_{ij} \boldsymbol{\theta}'_i \right).\end{aligned}$$

If the neighbor j is a master node, i.e., $\Sigma_{\text{ext},ji}^{-1} = \text{diag}(\infty, \infty)$, the parameters reduce to

$$\begin{aligned}\Sigma_{\text{in},ij}^{-1} &= \mathbf{A}_{ij}^T \mathbf{A}_{ij} \\ \Sigma_{\text{in},ij}^{-1} \boldsymbol{\mu}_{\text{ext},ji} &= \mathbf{A}_{ij}^T \mathbf{B}_{ij} \boldsymbol{\mu}_{\text{ext},ji}.\end{aligned}$$

For the parameters in (17) we utilized the generic formula for multiplying Gaussian normal distributions:

$$\prod_i \mathcal{N}_{\mathbf{x}}(\boldsymbol{\mu}_i, \Sigma_i) \propto \mathcal{N}_{\mathbf{x}}(\boldsymbol{\mu}, \Sigma) \quad (33)$$

with $\Sigma^{-1} = \sum_i \Sigma_i^{-1}$ and $\Sigma^{-1} \boldsymbol{\mu} = \sum_i \Sigma_i^{-1} \boldsymbol{\mu}_i$.

D. Mean Field Update Rules

Derivation of the message parameters for $m_{p_{ij} \rightarrow \theta'_i}(\boldsymbol{\theta}_i)$ in (25):

$$\begin{aligned}m_{p_{ij} \rightarrow \theta'_i}(\boldsymbol{\theta}'_i) &= \exp \left(\int \log(p_{ij}(\boldsymbol{\theta}'_{ij})) b_j(\boldsymbol{\theta}'_j) d\boldsymbol{\theta}'_j \right) \\ &\propto \exp \left(-\frac{1}{\sigma_m^2} \int \|\mathbf{A}_{ij} \boldsymbol{\theta}'_i + \mathbf{B}_{ij} \boldsymbol{\theta}'_j\|^2 \times \right. \\ &\quad \left. \mathcal{N}_{\boldsymbol{\theta}'_j}(\boldsymbol{\mu}_j, \Sigma_j) d\boldsymbol{\theta}'_j \right) \\ &\propto \exp \left(-\frac{1}{\sigma_m^2} \left(\boldsymbol{\theta}'_i{}^T \mathbf{A}_{ij}^T \mathbf{A}_{ij} \boldsymbol{\theta}'_i + \boldsymbol{\theta}'_i{}^T \mathbf{A}_{ij}^T \mathbf{B}_{ij} \boldsymbol{\mu}_j \right) \right) \\ &\propto \mathcal{N}_{\boldsymbol{\theta}'_i}(\boldsymbol{\mu}_{\text{in},ij}, \Sigma_{\text{in},ij})\end{aligned}$$

with the parameters (27) and (28). The message parameters of (26) are derived equivalently to (33).

REFERENCES

- [1] O. Hlinka, F. Hlawatsch, and P. M. Djuric, "Distributed particle filtering in agent networks: A survey, classification, and comparison," *IEEE Signal Process. Mag.*, vol. 30, pp. 61–81, Jan. 2013.
- [2] J. Elson and K. Römer, "Wireless sensor networks: a new regime for time synchronization," *SIGCOMM Comput. Commun. Rev.*, vol. 33, pp. 149–154, Jan. 2003.
- [3] I. Demirkol, C. Ersoy, and F. Alagoz, "MAC protocols for wireless sensor networks: a survey," *IEEE Commun. Mag.*, vol. 44, pp. 115–121, Apr. 2006.
- [4] S. Jagannathan, H. Aghajan, and A. Goldsmith, "The effect of time synchronization errors on the performance of cooperative MISO systems," in *IEEE GlobeCom Workshops 2004*, pp. 102–107, Nov. 2004.
- [5] D. W. Allan, "Time and frequency (time-domain) characterization, estimation, and prediction of precision clocks and oscillators," *Ultrasonics, Ferroelectrics and Frequency Control, IEEE Transactions on*, vol. 34, pp. 647–654, Nov. 1987.
- [6] O. Simeone, U. Spagnolini, Y. Bar-Ness, and S. H. Strogatz, "Distributed synchronization in wireless networks," *IEEE Signal Process. Magazine*, vol. 25, pp. 81–97, Sept. 2008.
- [7] Y.-C. Wu, Q. M. Chaudhari, and E. Serpedin, "Clock synchronization of wireless sensor networks," *IEEE Signal Process. Magazine*, vol. 28, pp. 124–138, Jan. 2011.
- [8] M. Maróti, B. Kusy, G. Simon, and A. Lédeczi, "The flooding time synchronization protocol," in *Proc. 2nd Int. Conf. on Embedded networked sensor systems*, New York, NY, USA, pp. 39–49, ACM, Nov. 2004.
- [9] P. Loschmidt, R. Exel, A. Nagy, and G. Gaderer, "Limits of synchronization accuracy using hardware support in ieee 1588," in *IEEE Int. Symp. Prec. Clock Synch.*, pp. 12–16, Sept. 2008.
- [10] A. Ahmad, D. Zennaro, E. Serpedin, and L. Vangelista, "A factor graph approach to clock offset estimation in wireless sensor networks," *IEEE Trans. Inform. Theory*, vol. 58, pp. 4244–4260, July 2012.
- [11] I. Skog and P. Händel, "Synchronization by two-way message exchanges: Cramér-Rao bounds, approximate maximum likelihood, and offshore submarine positioning," *IEEE Trans. Signal Processing*, vol. 58, pp. 2351–2362, Apr. 2010.
- [12] K.-L. Noh, Q. M. Chaudhari, E. Serpedin, and B. W. Suter, "Novel clock phase offset and skew estimation using two-way timing message exchanges for wireless sensor networks," *IEEE Trans. Commun.*, vol. 55, pp. 766–777, Apr. 2007.
- [13] M. Leng and Y.-C. Wu, "On clock synchronization algorithms for wireless sensor networks under unknown delay," *IEEE Trans. Veh. Technol.*, vol. 59, pp. 182–190, Jan. 2010.
- [14] R. T. Rajan and A.-J. van der Veen, "Joint motion estimation and clock synchronization for a wireless network of mobile nodes," in *Proc. IEEE Int. Conf. Acoustics, Speech, and Signal Processing*, pp. 2845–2848, May 2012.
- [15] L. Schenato and F. Fiorentin, "Average timesynch: A consensus-based protocol for clock synchronization in wireless sensor networks," *Automatica*, vol. 47, pp. 1878–1886, Sept. 2011.
- [16] T. Erseghe, D. Zennaro, E. Dall'Anese, and L. Vangelista, "Fast consensus by the alternating direction multipliers method," *IEEE Trans. Signal Processing*, vol. 59, pp. 5523–5537, Nov. 2011.
- [17] D. Zennaro, E. Dall'Anese, T. Erseghe, and L. Vangelista, "Fast clock synchronization in wireless sensor networks via ADMM-based consensus," in *Proc. 9th Int. Symp. Model. Optim. Mobile, Ad Hoc, Wireless Netw.*, pp. 148–153, May 2011.
- [18] R. Solis, V. Borkar, and P. Kumar, "A new distributed time synchronization protocol for multihop wireless networks," in *Proc. 45th IEEE Conf. Decis. Control*, pp. 2734–2739, Dec. 2006.
- [19] J. Elson, L. Girod, and D. Estrin, "Fine-grained network time synchronization using reference broadcasts," in *Proc. 5th Symp. Operat. Syst. Design Implement.*, pp. 147–163, Dec. 2002.
- [20] M. Leng and Y.-C. Wu, "Distributed clock synchronization for wireless sensor networks using belief propagation," *IEEE Trans. Signal Processing*, vol. 59, pp. 5404–5414, Nov. 2011.
- [21] N. Freris, V. Borkar, and P. Kumar in *Proc. 45th IEEE Conf. Decis. Control*, pp. 5744–5749, Dec. 2009.
- [22] R. Olfati-saber, J. A. Fax, and R. M. Murray, "Consensus and cooperation in networked multi-agent systems," in *Proc. IEEE*, vol. 1, pp. 215–233, Jan. 2007.
- [23] F. Kschischang, B. Frey, and H.-A. Loeliger, "Factor graphs and the sum-product algorithm," *IEEE Trans. Inform. Theory*, vol. 47, pp. 498–519, Feb. 2001.
- [24] J. Zheng and Y.-C. Wu, "Joint time synchronization and localization of an unknown node in wireless sensor networks," *IEEE Trans. Signal Processing*, vol. 58, pp. 1309–1320, Mar. 2010.
- [25] H. L. van Trees, *Detection, Estimation, and Modulation Theory: Radar-Sonar Signal Processing and Gaussian Signals in Noise*. Melbourne, FL, USA: Krieger Publishing Co., Inc., 1992.
- [26] H. Wymeersch, J. Lien, and M. Z. Win, "Cooperative localization in wireless networks," *Proc. IEEE*, vol. 97, pp. 427–450, Feb. 2009.
- [27] J. S. Yedidia, W. T. Freeman, and Y. Weiss, "Constructing free energy approximations and generalized belief propagation algorithms," *IEEE Trans. Inform. Theory*, vol. 51, pp. 2282–2312, July 2005.
- [28] J. Dauwels, "On variational message passing on factor graphs," *Proc. IEEE Int. Symp. Inf. Theory*, pp. 2546–2550, June 2007.
- [29] Y. Weiss and W. T. Freeman, "Correctness of belief propagation in gaussian graphical models of arbitrary topology," *Neural Computation*, vol. 13, pp. 2173–2200, Oct. 2001.
- [30] D. M. Malioutov, J. K. Johnson, and A. S. Willsky, "Walk-sums and belief propagation in gaussian graphical models," *Journal of Machine Learning Research*, vol. 7, pp. 2031–2064, 2006.
- [31] C. M. Bishop, *Pattern Recognition and Machine Learning (Information Science and Statistics)*. Secaucus, NJ, USA: Springer-Verlag New York, Inc., 2006.
- [32] M. J. Wainwright and M. I. Jordan, "Graphical models, exponential families, and variational inference," *Found. Trends Mach. Learn.*, vol. 1, pp. 1–305, Jan. 2008.